Heat protective properties of enclosure structure from thin-wall profiles with foamed concrete

V.A. Rybakov[a]*, I.A. Ananeva[b], E.D. Pichugin[c], M. Garifullin[d]
[a] *Peter the Great St. Petersburg Polytechnic University, St.-Petersburg, Russia*
[b] *OTSK, Ltd, St.-Petersburg, Russia*
[c] *«Airline», Moscow, Russia*
[d] *Tampere University, Tampere, Finland*
* E–mail: fishermanoff@mail.ru

Abstract. Receiving the qualitative, energy efficient and economic building is the main tendency in the civil engineering. One of the leading places is occupied by technology of frame-panel construction with use of new non-autoclaved, monolithic foamed concrete technology producing on a building site. On the example of the real samples there were determined the heat-shielding properties of foamed concrete in a condition of setting process and after attainment of strength with a practical and theoretical methods. The results were obtained for a non-autoclaved monolithic foamed concrete wall fragment (lightweight steel concrete structure – LSCS) for the areas with and without rigid reinforcement with steel thin-wall profiles (lightweight gauge steel structure – LGSS). Influence of the thermal bypass on cold-resisting properties of enclosure structures with technology "Intech LB" is revealed. On the basis of the received results, modernization of a design for improvement of its thermotechnical characteristics is made.

1. Introduction

Construction of residential country house or cottage is often associated with significant expenses; however, integration of new materials and modern technologies allows decrease them.

Technology that combines well known frame-panel construction technology (timber, plastic and thin-walled steel structures) with modern technology of construction site production of non-autoclave, cast in-situ, acoustic and thermal insulating, constructive foamed concrete can be considered as breakthrough in modern low-rise construction industry. Application of such concrete gives an opportunity to decrease shipping costs, construction period, materials consumption. Moreover, even thin foamed concrete walls possess sufficient thermal insulation properties. High mobility of this concrete type allows to effortlessly perform concrete mix distribution and to form building structures on any height.

There is a large variety of thermal insulating materials in modern construction industry; such as mineral wool, polystyrene and polyurethane foam. For example, M.V. Leshchenko and V.A. Semko proposes to use polystyrene concrete as an insulating material in wall panels made of light gauge studs. It should solve the problem of thermal bridges in such panels [1].

However, they possess significant disadvantages. For instance, mineral wool insulators are subjected to sitting and, also, moisturizing that causes in one hand decrease of insulating properties, in another cause increase in load that is crucial in rooftop insulation. Cellular concretes are well known as material for a long time and develop as foamed and aerated concretes. These branches are described in article [2–6].

Thermal insulation of building enclosing by cast in-situ foamed concrete is relatively modern way of cellular concrete application. This technology is developed and integrated in Russian Federation construction industry by group of V.D. Vasiliev [7, 8].

A.Y. Struchkova, Yu.G. Barabanshikov, K.S. Semenov, A.A. Shaibakova solved the problems of thermal cracking resistance of massive concrete and reinforced concrete structures during the building period are

considered. The calculation results of a research on the effect of hardening temperature on the process of heat dissipation process of concrete are given [9].

T.V. Krivaltzevich and E.V. Gurova conducted comparison of technical properties and basic characteristics of thermal insulation materials of different structure and considered advantages and disadvantages of non-autoclave foamed concrete in their work [10].

V.V. Bespalov, D. Ucer, I.D. Salmanov, I.N. Kurbamov, S.V. Kupavykh consider a problem whose purpose is determine the combined behavior of masonry walls and reinforcing meshes together, according to their deformation characteristics. The results obtained from the theoretical sample wall and the case study wall with plain and reinforced alternatives stated that the compatibility of deformation characteristics between the wall and the reinforcing mesh is the key for combined strength behavior of the wall [11].

V.V. Plotnikov and M.V. Bogatovsky demonstrated research results of development of energy and material saving technology of construction of interior multilayer cast in-situ walls with application of low density composite foamed concretes [12]. This technology provides ability to control formation of foamed concrete structure in process of its obtainment and on first stages of curing. For example, in articles [13–17] possibility of direction of pore structure of non-autoclave foam concrete is studied. Option of concrete performance characteristics increase by adding of different admixtures (colloidal suspension of silicon dioxide, cold-bonded fly ash, etc). Such admixture stabilizes and improves pore structure of material, developing properties of foamed concrete. Also, the article [18] proposes a numerical model for estimating the effect of composite reinforcement on the bearing capacity of a compressed-bent masonry wall which is constructed on the basis of experimental studies of walls from cellular concrete blocks.

Nowadays, there are technologies of enclosing structures construction based on combination of light steel framing and various thermal insulators. Lightweight metal framing is used for constructive purposes worldwide. However, it is applied in Russia for low rise construction only, since lack of production standards.

Major advantages of light steel framing constructions are demonstrated in articles [19–23].

D.V. Kuzmenko and N.I. Vatin [24] developed new type of enclosing structure based on light meal framing – thermal panel. Main components are thermal profile and efficient thermal insulator. Thermal panel is perspective modern energy-saving technology that can be applied in high-rise construction.

Based on LSTK M.K. Bronzova, N.I. Vatin, M.R. Garifullin were engaged in studying of a design in the work [25] and others in works [26–32].

Application of modern constrictions is reasonable only if their superior thermal properties exploited properly. Results of reduced total thermal resistance calculation and heat transfer performance uniformity factor determination are demonstrated in work [33], performed by T.A. Karnilov and G.N. Gerasimov. They concluded that the most efficient method of thermal protection of two-layer walls is variation exterior layer along with constant width of inner layer that corresponds to minimal parameter of pillar cross section, determined by obtained value of bearing capacity.

Enclosing structure, applying in low-rise construction and in attic erection, is chosen as object of research. The structure consists from galvanized steel profile TS200-50-1.5, filled with non-autoclave cast in-situ foamed concrete in condition of natural moist contain (D200, 300 mm). Object was tested in climate chamber to determine thermal technical properties of construction.

Results of wall fragment thermal technical properties evaluation by climate chamber presented in article [34]. Temperature values on wall-slab joint (thermal conductive location) have been determined and compared to values calculated according to calculated values of temperature and dew point parameters.

There are developed three Standards that set regulations for design and construction cast in-situ, non-autoclave foamed concrete buildings. Saint-Petersburg Peter the Great Polytechnic University research group (N.I. Vatin, V.A. Rybakov, and A.O. Rodicheva) developed Company's Code

1) STO 83835311.001-2015. Reinforced concrete structures from heat-insulating non-autoclave monolithic foam concrete with rigid reinforcement from profile steel, with facing with asbestos-cement and glass-magnesite sheets. Design rules. ("Monplaisir", Ltd., Russia)

2) STO 06041112.001–2018 (changed 10.02.2019). Panels from steel concrete structures based on heat-insulating non-autoclave monolithic foam concrete, profile steel faced with fibrocement sheets. ("INTECH LB", Ltd., Russia)

3) STO 06041112.002–2018 (changed 10.02.2019). Steel concrete structures from heat-insulating non-autoclave monolithic foam concrete, profile steel with facing with fibrocement cement sheets. Design rules. ("INTECH LB", Ltd., Russia)

Requirements for cast in-situ foamed concrete are based on STO 83835311.001-2015, STO 06041112.001-2018, and STO 06041112.002-2018 and developed by Saint-Petersburg Peter the Great Polytechnic University research group.

Rybakov, V.A., Ananeva, I.A., Pichugin, E.D., Garifullin, M.

12

Foamed concrete is a widely applicable material due to its economic efficiency. Main drawback of this material – low mechanical strength can be coped with framework for construction. Lightweight steel framing from thin wall profiles is one of the most convenient option for this purpose.

This research is focused on determination of thermal protecting properties of non-autoclave cast in-situ foamed concrete after strength gain in reinforced and unreinforced sections of enclosing structure, consisting of steel thin-wall profiles framing and cast in-situ foamed concrete.

Research process can be divided on solution of three goals:

1. Determination of physical and mechanical properties of foamed concrete- used in research;

2. Determination of thermal protecting properties of bearing enclosing structures, consisting of steel thin-walled profiles and cast in-situ foamed concrete;

3. Comparison of thermal resistance values in reinforced and unreinforced sections of structure.

2. Methods

2.1. Determination of thermal and mechanic parameters of thermal insulating constructive material

2.1.1. Determination of humidity

Humidity of foamed concrete is determined according to Russian State Standard GOST 12730.2–78. Twelve samples (100×100×100 mm) have been weighted in moist condition, put in low temperature experimental furnace SNOL 67/350 and being dried (+105 °C) until mass can be considered constant (approximately 48 hours). Then dry samples being weighted again and humidity being calculated by formula (1):

$$W_m = \frac{m_b - m_c}{m_c} \cdot 100 \text{ \%},$$

(1)

where W_m is samples humidity, %;

m_b is mass of samples before drying, kg;

m_c is mass of samples after drying, kg.

2.1.2. Determination of density

1. Density is found by formula (2):

$$\rho = \frac{m}{V},$$

(2)

where ρ is density, kg/m³;

m is mass, kg;

V is volume, m^3.

Results of density and humidity determination are presented in Table 1.

Table 1. Density and humidity of samples.

Samples number	Mass of moist samples, kg	Density, kg/m³	Mass of dry samples, kg	Humidity, %
1	0.497	497	0.342	45
2	0.441	441	0.307	44
3	0.458	458	0.32	43
4	0.466	466	0.327	43
5	0.472	472	0.36	43
6	0.511	511	0.33	42
7	0.469	469	0.327	42
8	0.46	460	0.307	41
9	0.44	440	0.331	43
10	0.441	441	0.306	44
11	0.502	502	0.348	44
12	0.624	624	0.438	42
Average value	–	481.75	0.337	43

Rybakov, V.A., Ananeva, I.A., Pichugin, E.D., Garifullin, M.

2.1.3. Determination of strength

Each specimen is being tested by compact experimental press MIP-25/50 to evaluate compressive strength. Samples 2, 4, 6, 11 have been put in plastic containers to conserve dehydrated condition after drying in SNOL 67/350 furnace. Samples 1, 3, 8, 12 were tested in conditions of natural humidity; mass of these Samples raised by 3–5 grams since furnace extraction. Results presented in Table 2.

Table 2. Compressive strength of specimens.

Samples number	Humidity, %	Mass, kg	Compressive strength, MPa
1	1	0.346	0.1
2	0.1	0.307	0.14
3	1	0.323	0.15
4	0.1	0.327	0.1
6	0.1	0.36	0.19
8	1	0.331	0.12
11	0.1	0.348	0.16
12	1	0.443	0.12
		Average value	0.135

2.2. Determination of thermal protecting properties of enclosing structure based on thin-wall steel C-beams and cast in-situ foamed concrete.

Structure consists from non-autoclave cast in-situ foamed concrete D200 block (460×760×300 mm) with natural humidity (tests performed 37 days after casting) and two galvanized steel C-beams PS 200-50-1.5 (Figure 1).
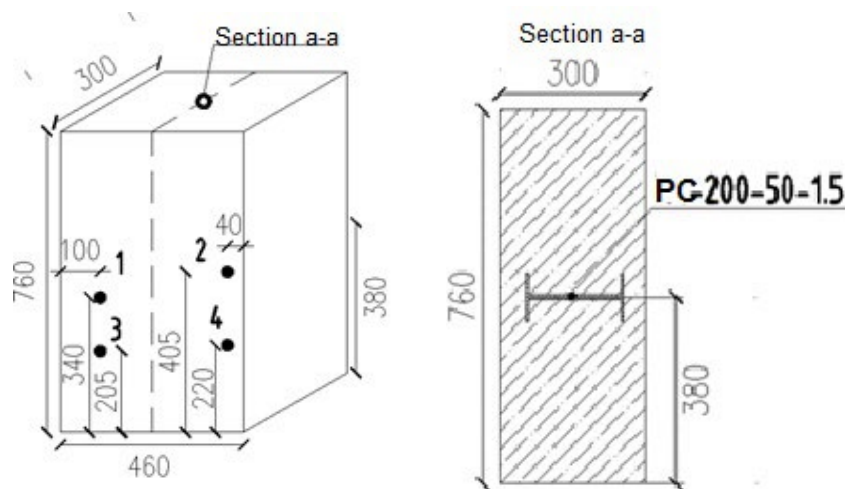
Figure 1. Geometric parameters of samples. Location of temperature sensors.

Goals of the experiment are determination of thermal resistance in points of reinforced and unreinforced foamed concrete, their comparison and analytic comparison of actual resistance to thermal transition to structure with theoretic calculation for the samples.

2.2.1. Determination of thermal technical properties of enclosing structure, climate chamber tests

Structure has been put in climate chamber TX-500, with following temperature conditions: temperature in cold (exterior) section is set on –30 °C, temperature in warm (interior) section) set on +24 °C. The sample was subjected to chamber tests until installation of thermal process balance, in this case – 3 days. Temperature sensors and sensors of heat flow were installed on surface of the sample (Figure 1). Results are formed in Table 2. Charts that represent dependence of surface temperature om time and dependence of heat flow on time presented on Figures 3, 4.

Coefficient of thermal conductivity is determined by formula (3):

Results of coefficient of thermal conductivity calculation put in Table 4. Approximate value is calculated for each point after installation of thermal balance, in this case balance was set on 4:57 07.06.2017.

Rybakov, V.A., Ananeva, I.A., Pichugin, E.D., Garifullin, M.

Table 3. Temperature value sand heat flows values in interior and exterior points of wall samples.

Date	Time	Point 1			Point 2		
Day/ month/year	Hour/minute	Heat flow W/m²	Interior temp., °C	Exterior temp., °C	Heat flow W/m²	Interior temp., °C	Exterior temp., °C
05.05.	16:57	10.733	21.61	23.17	6.776	23.09	23.3
05.05.	19:57	34.892	18.01	−26.26	26.205	20.95	−25.8
05.05.	22:57	41.942	17.2	−26.53	41.693	20.14	−26.44
06.05.	1:57	46.919	17.02	−26.68	50.544	19.88	−26.72
06.05.	4:57	52.112	17.19	−26.69	54.82	20.02	−26.8
06.05.	7:57	52.868	17.77	−26.76	62.061	20.59	−26.87
06.05.	10:57	51.413	17.98	−26.9	62.293	20.75	−27.01
06.05.	13:57	53.769	18.58	−26.9	64.086	21.36	−27.03
06.05.	16:57	51.638	18.38	−26.96	62.781	21.06	−27.13
06.05.	19:57	50.962	17.96	−26.91	60.947	20.55	−27.1
06.05.	22:57	52.152	17.69	−26.94	65.48	20.29	−27.07
07.05.	1:57	49.82	17.65	−26.89	62.974	20.26	−27.06
07.05.	4:57	56.092	17.85	−26.93	64.895	20.37	−27.12
07.05.	7:57	57.965	20.93	−26.99	73.648	23.5	−27.1
07.05.	10:57	51.404	19.92	−27.11	68.787	22.42	−27.27
07.05.	13:57	49.483	19.75	−27.13	71.43	22.29	−27.22
07.05.	16:57	52.964	19.39	−27.02	68.723	21.85	−27.12
07.05.	19:57	49.829	18.72	−26.91	65.984	21.08	−27.02
07.05.	22:57	48.752	18.51	−26.99	71.406	20.93	−27.14
08.05.	1:57	49.941	18.62	−26.91	68.676	20.96	−27.06
08.05.	4:57	52.369	18.78	−27.03	68.26	21.05	−27.11
08.05.	7:57	58.463	21.09	−26.96	72.279	23.49	−27.09
08.05.	10:57	57.764	23.63	−27.15	77.732	26.05	−27.18
08.05.	13:57	60.24	20.84	−27.09	64.07	23.17	−27.13
08.05.	16:57	54.548	19.88	−27.09	67.018	22.26	−27.12

Date	Time	Point 3		Point 4			
Day/ month/year	Hour/minute	Heat flow W/m²	Interior temp., °C	Day/ month/year	Hour/minute	Heat flow W/m²	Interior temp., °C
05.05.	16:57	16.194	21.19	22.47	24.958	21.87	22.81
05.05.	19:57	19.387	19.43	−25.67	28.275	21	−24.48
05.05.	22:57	30.154	18.79	−26.09	35.133	20.89	−25.25
06.05.	1:57	31.402	18.5	−26.31	40.217	20.99	−25.53
06.05.	4:57	43.019	18.66	−26.34	41.656	21.32	−25.67
06.05.	7:57	38.47	19.19	−26.48	47.48	22.07	−25.79
06.05.	10:57	40.138	19.36	−26.68	44.839	22.32	−26.01
06.05.	13:57	39.028	19.92	−26.71	44.083	22.98	−26.08
06.05.	16:57	37.171	19.73	−26.8	42.373	22.69	−26.16
06.05.	19:57	44.586	19.3	−26.73	42.866	22.23	−26.13
06.05.	22:57	36.372	19.09	−26.74	42.126	22.03	−26.16
07.05.	1:57	35.581	19.09	−26.72	41.982	22.04	−26.09
07.05.	4:57	39.412	19.26	−26.76	41.021	22.22	−26.09
07.05.	7:57	41.009	22.19	−26.84	43.256	25.44	−26.23
07.05.	10:57	43.729	21.33	−27.04	42.644	24.39	−26.35
07.05.	13:57	35.995	21.2	−27.01	43.725	24.21	−26.35
07.05.	16:57	36.518	20.88	−26.91	41.227	23.76	−26.27
07.05.	19:57	34.021	20.2	−26.82	39.27	23.05	−26.17
07.05.	22:57	36.858	19.98	−26.88	40.256	22.95	−26.24
08.05.	1:57	40.124	20.1	−26.81	39.453	22.98	−26.18
08.05.	4:57	36.097	20.17	−26.98	38.776	23.09	−26.22
08.05.	7:57	40.893	22.58	−26.89	42.882	25.62	−26.25
08.05.	10:57	43.737	25.08	−27.04	46.096	28.25	−26.43
08.05.	13:57	37.199	22.36	−26.99	37.424	25.23	−26.31
08.05.	16:57	35.843	21.45	−26.98	38.999	24.34	−26.28

Used next formulas from ISO 7345:1987 Thermal insulation – Physical quantities and definitions (MOD), determine coefficient of thermal conductivity:

Rybakov, V.A., Ananeva, I.A., Pichugin, E.D., Garifullin, M.

15

$$R = \frac{T_2 - T_1}{q};$$

$$\lambda = \frac{q \cdot d}{T_2 - T_1},$$

(3)

where λ is coefficient of thermal conductivity, W/(m·K);

q is heat flow, W/m²;

d is wall thickness, m;

T_1, T_2 are temperature of wall surfaces, °C

Table 4. Coefficient of thermal conductivity of surface.

Date Day/month/year	Time Hour/minute	Coefficient of thermal conductivity, W/(m·K)			
Date	Time	Point 1	Point 2	Point 3	Point 4
07.05.	4:57	0.376	0.41	0.257	0.255
07.05.	7:57	0.363	0.437	0.251	0.251
07.05.	10:57	0.328	0.415	0.271	0.252
07.05.	13:57	0.317	0.433	0.224	0.259
07.05.	16:57	0.342	0.421	0.229	0.247
07.05.	19:57	0.328	0.412	0.217	0.239
07.05.	22:57	0.321	0.446	0.236	0.246
08.05.	1:57	0.329	0.429	0.257	0.241
08.05.	4:57	0.343	0.425	0.23	0.236
08.05.	7:57	0.365	0.429	0.248	0.248
08.05.	10:57	0.341	0.438	0.252	0.253
08.05.	13:57	0.377	0.382	0.226	0.218
08.05.	16:57	0.348	0.407	0.222	0.231
Average value		0.344	0.422	0.24	0.244

Technical thermal resistance is calculated by formula (4) (For reinforced section is R_a, for unreinforced section is R_b).
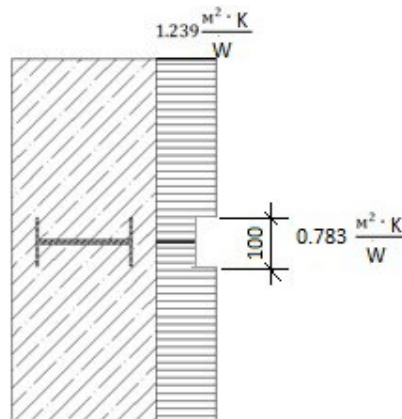
$$R = \frac{d}{\lambda},$$

(4)

where R is thermal resistance, (m²·K)/W;

d is wall thickness, m;

λ is coefficient of thermal conductivity, W/(m·K)

$$R_a = \frac{0.3}{0.383} = 0.783 \frac{m^2 \cdot K}{W}; \quad R_b = \frac{0.3}{0.242} = 1.239 \frac{m^2 \cdot K}{W}.$$

Thermal resistance diagram for sample section is plotted to calculate thermal resistance for whole construction (Figure 2).

Figure 2. Thermal conductivity resistance for specimen cross section.

Rybakov, V.A., Ananeva, I.A., Pichugin, E.D., Garifullin, M.

Average value of thermal resistance is calculated:

$$R = \frac{A_1 + A_2 + A_3 \ldots + A_n}{\dfrac{A_1}{R_1} + \dfrac{A_2}{R_2} + \dfrac{A_3}{R_3} + \ldots \dfrac{A_n}{R_n}} = 1.209 \, \frac{m^2 \cdot K}{W}. \tag{5}$$

Formula (6) is applied to obtain thermal conductivity:

$$R_o = \frac{1}{\alpha_e} + R + \frac{1}{\alpha_i}, \tag{6}$$

where α_i is heat exchange coefficient for interior surface of enclosure structure by Set of Rules 50.13330.2012 $(\alpha_i = 8.7 \, \dfrac{m^2 \cdot K}{W})$;

α_e is heat exchange coefficient for exterior surface of enclosure structure by Set of Rules 50.13330.2012 $(\alpha_e = 23 \, \dfrac{m^2 \cdot K}{W})$;

R is thermal resistance, (m²·K)/W.

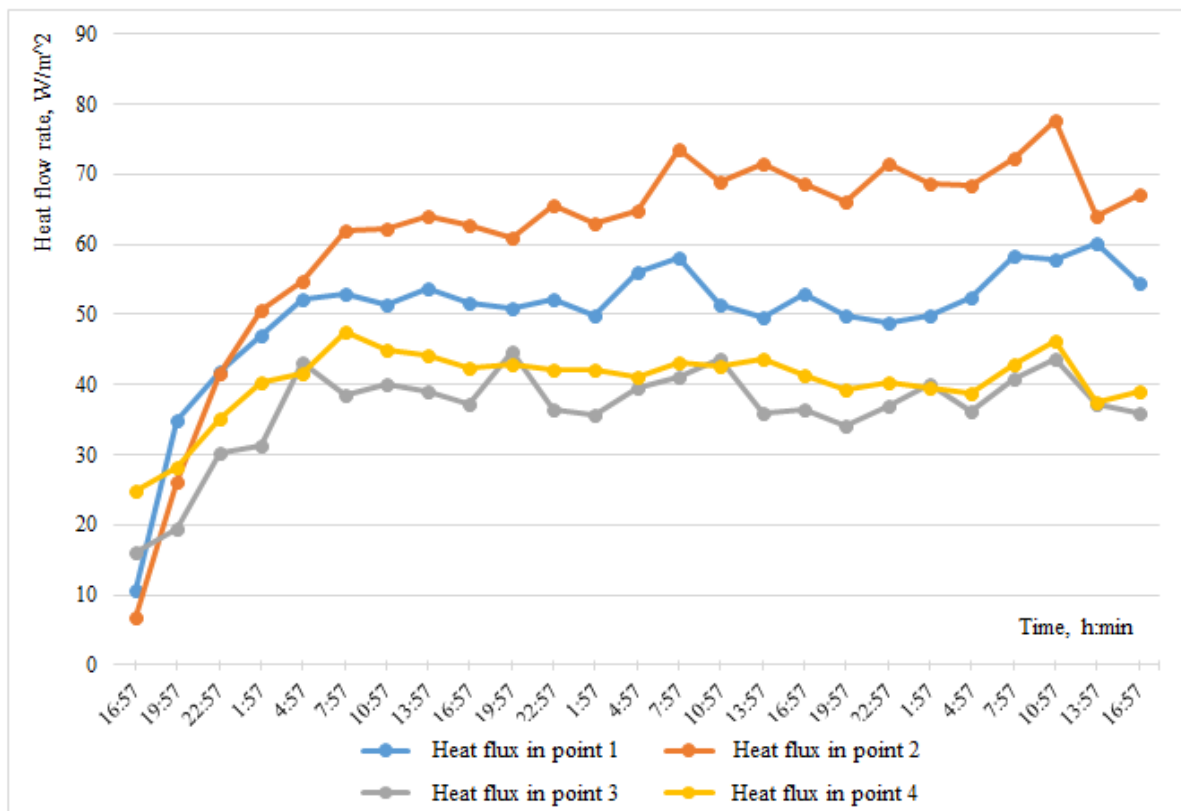$$R_o = \frac{1}{8.7} + 1.209 + \frac{1}{23} = 1.367 \, \frac{m^2 \cdot K}{W}.$$

Figure 3. Heat flow chart.

3. Results and Discussion

Technologies of cast in situ non-autoclave foamed concrete buildings construction are lack in Russian industry in 2020. Thus, Business association "SOVBI" is a unique manufacturer of bearing enclosing structures, based on thin-wall profile metal framing and cast in situ foamed concrete. Therefore, research from this article does not have any analogue, and consideration of comparison of obtained results with others is premature. Researches of thermal-saving properties of this kind of structures are also lack abroad.

However, in order to evaluate adequacy of obtained results, method from ISO_06946–2007 can be applied.

Rybakov, V.A., Ananeva, I.A., Pichugin, E.D., Garifullin, M.

3.1. Theoretical calculation of thermal conductivity resistance for non-uniform enclosing structure

Calculation of thermal conductivity resistance for non-uniform enclosing structure is performed according to following rules ISO_06946–2007.

The total thermal resistance R_o, of a component consisting of thermally homogeneous and thermally inhomogeneous layers parallel to the surface is calculated as the arithmetic mean of the upper and lower limits of the resistance:

$$R_o = \frac{R_T' + R_T''}{2}, \tag{7}$$

where R_T' is the upper limit of the total thermal resistance, is determined by formula:

$$\frac{1}{R_T'} = \frac{f_a}{R_{Ta}} + \frac{f_b}{R_{Tb}} + \frac{f_c}{R_{Tc}} + \frac{f_d}{R_{Td}} + \frac{f_e}{R_{Te}}. \tag{8}$$

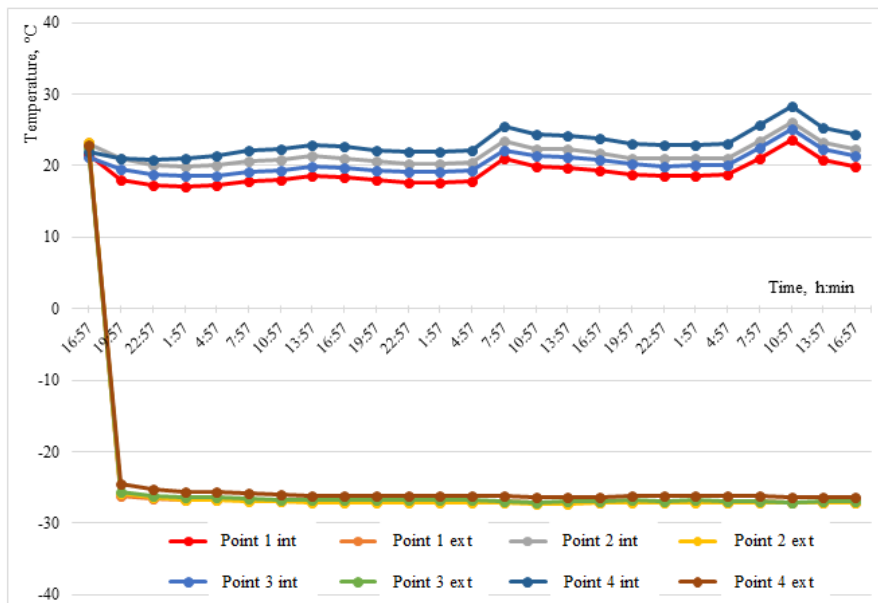$f_a; f_b; f_c; f_d; f_e$ are fractional area of each section (Figure 5).

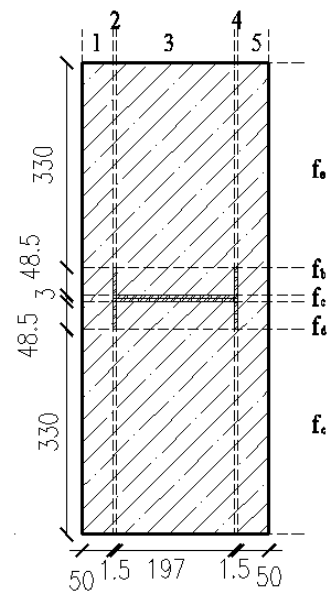**Figure 4. Surface temperature chart.**   **Figure. 5 Division to planes.**

$R_{Ta}; R_{Tb}; R_{Tc}; R_{Te}$ are the total thermal resistances from environment to environment for each section, calculated using Equation (4).

$$\frac{1}{R_T'} = 2 \cdot \frac{0.33}{\frac{0.3}{0.08}} + 2 \cdot \frac{0.0485}{2 \cdot \frac{0.05}{0.08} + 2 \cdot \frac{0.0015}{47} + \frac{0.197}{0.08}} + \frac{0.003}{2 \cdot \frac{0.05}{0.08} + \frac{0.2}{47}} = \frac{1}{0.44} \frac{m^2 \cdot K}{W}.$$

R_T'' is the lower limit of the total thermal resistance:

Calculate an equivalent thermal resistance, R_j, for each thermally inhomogeneous layer using Equation (9):

$$\frac{1}{R_j} = \frac{f_a}{R_{aj}} + \frac{f_b}{R_{bj}} + \frac{f_c}{R_{cj}} + \frac{f_d}{R_{dj}} + \frac{f_e}{R_{ej}}. \tag{9}$$

The lower limit is then determined using Equation (10):

$$R_T'' = R_1 + R_2 + R_3 + R_4 + R_5. \tag{10}$$

Determine $\dfrac{1}{R_j}$ for every layer with Equation (9):

Rybakov, V.A., Ananeva, I.A., Pichugin, E.D., Garifullin, M.

18

$$\frac{1}{R_1} = \frac{0.33 + 0.0485 + 0.003 + 0.00485 + 0.33}{\dfrac{0.05}{0.08}} = 1.216 \frac{W}{m^2 \cdot K};$$

$$\frac{1}{R_2} = 2 \cdot \frac{0.33}{\dfrac{0.0015}{0.08}} + \frac{0.0485 + 0.003 + 0.0485}{\dfrac{0.0015}{47}} = 3168.2 \frac{W}{m^2 \cdot K};$$

$$\frac{1}{R_3} = 2 \cdot \frac{0.3785}{\dfrac{0.197}{0.08}} + \frac{0.003}{\dfrac{0.197}{47}} = 1.023 \frac{W}{m^2 \cdot K}.$$

$\dfrac{1}{R_1} = \dfrac{1}{R_5}$ and $\dfrac{1}{R_2} = \dfrac{1}{R_4}$ as the layers are similar, thus:

$$R''_T = 2.62 \frac{m^2 \cdot K}{W};$$

$$R_o = \frac{2.27 + 2.62}{2} = 2.44 \frac{m^2 \cdot K}{W}.$$

4. Conclusions

1. Research shows that strength properties of material do not allow to evaluate concrete with axial compression strength class, thus impact of foamed concrete on composite mechanical strength is negligibly. Major function of foamed concrete is thermal insulation.

2. Identified thermal protective properties of composite structure made of foamed concrete and steel thin-wall profiles have been determined experimentally in sections with/without reinforcement: reinforced sections – 0.783 (m²·K)/W; unreinforced sections – 1.239 (m²·K)/W

3. It's established that the heat resistance of the enclosing structure in reinforced section is 63 % of resistance in unreinforced one.

4. Shown comparison of thermal conductivity resistance of non-uniform enclosing structure has been performed by experimental and theoretical methodic :thermal conductivity resistance of enclosure, obtained experimentally – 1.367(m²·K)/W; thermal conductivity resistance of enclosure, obtained by calculation – 2.44(м²·K)/W.

5. It's established that the heat resistance of the thermal conductivity of non-uniform enclosure, obtained experimentally is two times less than resistance, calculated theoretically.

6. It is recommended to modify enclosure made of steel thin-wall profiles and foamed concrete with layer of mineral wool for optimal heating performance according to requirements for Province of Leningrad.

7. Explanation of the discrepancies between the practical and theoretical values of the heat transmission resistance:

7.1 As we used monolithic foamed concrete on the site in the winter time, high probability that during the process of pouring of the sample, water or snow penetrated into the pores of sample and decrease heat transmission resistance.

7.2 Experimental accuracy.

5. Acknowledgment

References

1. Leshchenko, M.V., Semko, V. Thermal characteristics of the external walling made of cold-formed steel studs and polystyrene concrete. Magazine of Civil Engineering. 2015. 60(8). Pp. 44–55. (rus). DOI: 10.5862/MCE.60.6.
2. Korniyenko, S.V., Vatin, N.I., Gorshkov, A.S. Thermophysical field testing of residential buildings made of autoclaved aerated concrete blocks. Magazine of Civil Engineering. 2016. 64(4). Pp. 10–25. DOI: 10.5862/MCE.64.2
3. Gorshkov, A.S., Pestryakov, I.I., Korniyenko, S.V., Vatin, N.I., Olshevskiy, V.Ya. Actual thermal insulation properties of cellular autoclave curing concretes, Construction of Unique Buildings and Structures. 2018. 68(5). Pp. 75–104. (rus) DOI: 10.18720/CUBS.68.7
4. Korniyenko, S. Complex analysis of energy efficiency in operated high-rise residential building: case study. E3S Web of Conferences. 2018. No. 33. Pp. 02005.

Rybakov, V.A., Ananeva, I.A., Pichugin, E.D., Garifullin, M.

5. Korniyenko, S.V. The experimental analysis and calculative assessment of building energy efficiency. Applied Mechanics and Materials. 2014. Vol. 618. Pp. 509–513.

6. Barabanshchikov, Y., Fedorenko, I., Kostyrya, S., Usanova, K. Cold-Bonded Fly Ash Lightweight Aggregate Concretes with Low Thermal Transmittance. Advances in Intelligent Systems and Computing. 2019. 983. Pp. 858–866.

7. Lundyshev, I.A. Karkasnyye sistemy, primenyayemyye v ograzhdayushchikh konstruktsiyakh pri stroitel'stve iz monolitnogo penobetona [Frame systems used in enclosure structure in construction from monolithic autoclaved aerated concrete]. Magazine of Civil Engineering. 2009. 3(1). Pp. 13–16. (rus)

8. Vasilyev, V.D. Monolitnyy penobeton po tekhnologii «SOVBI» [Monolithic foam concrete according to the "Svbi" technology]. Stroitelnyye materialy. 2005. No. 12. Pp. 39–40. (rus)

9. Struchkova, A.Y., Barabanshchikov, Yu.G., Semenov, K.S., Shaibakova, A.A. Heat dissipation of cement and calculation of crack resistance of concrete massifs. Magazine of Civil Engineering. 2018. No. 78(2). Pp. 128–135. doi: 10.18720/MCE.78.10

10. Krivaltsevich, T.V., Gurova, Ye.V. Sravneniye neavtoklavnogo penobetona s drugimi teploizolyatsionnymi materialami [comparison of non-autoclave foam concrete with other heat-insulating materials]. Arkhitektura, stroitelstvo, transport. 2015. Pp. 508–512. (rus)

11. Bespalov, V.V., Ucer, D., Salmanov, I.D., Kurbanov, I.N., Kupavykh, S.V. Deformation compatibility of masonry and composite materials. Magazine of Civil Engineering. 2018. No. 78(2). Pp. 136–150. doi: 10.18720/MCE.78.11

12. Plotnikov, V.V., Botagovskiy, M.V. Povysheniye dolgovechnosti monolitnogo penobetona nizkoy plotnosti putem modifitsirovaniya tsementa aktivirovannymi kristallogidratami [Improving the durability of monolithic low-density foam concrete by modifying cement with activated crystalline hydrates]. Promyshlennoye i grazhdanskoye stroitelstvo. 2015. No. 10. Pp. 33–39. (rus)

13. Pertseva, O., Nikolskiy, S. Dependence of relative decreasing in strength by rate of strain for the new rapid method for determination of concrete frost resistance. Applied mechanics and materials. 2015. Pp. 505–510.

14. Korsun, V., Korsun, A. The influence of precompression on strength and strain properties of concrete under the effect of elevated temperatures. Applied mechanics and materials. 2015. Pp. 469–474.

15. Korsun, V., Vatin, N., Korsun, A., Nemova, D. Physical-mechanical properties of the modified fine-grained concrete subjected to thermal effects up to 200°s. Applied mechanics and materials. 2014. Pp. 1013–1017.

16. Usanova, K., Barabanshchikov, Yu., Fedorenko Yu., Kostyrya S. Cold-bonded fly ash aggregate as a coarse aggregate of concrete. Construction of Unique Buildings and Structures. 2018. 9(72). Pp. 31–45. DOI: 10.18720/CUBS.72.2

17. Bayev, M.N., Shchukina, Yu.V. Teploizolyatsionnyy neavtoklavnyy penobeton s povyshennymi kharakteristikami [Heat-insulating non-autoclave foam concrete with enhanced characteristics]. Polzunovskiy vestnik. 2011. No. 1. Pp. 35–37. (rus)

18. Orlovich, R.B., Bespalov, V.V., Derkach, V.N. Compressed-bent masonry walls reinforced with composite materials. Magazine of Civil Engineering. 2018. No. 79(3). Pp. 112–119. doi: 10.18720/MCE.79.12

19. Sovetnikov, D.O., Videnkov, N.V., Trubina, D.A. Light gauge steel framing in constructionof multi-storey buildings. Construction of Unique Buildings and Structures. 2015. 30(3). Pp. 152–165. (rus). DOI: 10.18720/CUBS.30.11

20. Rybakov, V.A., Molchanova, N., Laptev, V., Suslova, A., Sivokhin, A. The effect of conjunction flexibility on the local stability of steel thin-walled slab beams. MATEC Web of Conferences. 2016. Pp. 01017.

21. Trubina, D., Abdulaev, D.A., Pichugin, E., Rybakov, V., Garifullin, M., Sokolova, O. Comprasion of the bearing capacity of lst-profile depending on the thickness of its elements. Applied mechanics and materials. 2015. Pp. 752–757.

22. Trubina, D., Abdulaev, D., Pichugin, E., Rybakov, V. Geometric nonlinearity of the thin-walled profile under transverse bending. Applied mechanics and materials. 2014. Pp. 1133–1139.

23. Ariyanayagam, A.D., Poologanathan, K., Mahendran, M. Thermal modelling of load bearing cold-formed steel frame walls under realistic design fire conditions. Advanced Steel Construction. 2017. No. 2. Pp. 160–189.

24. Kuz'menko, D.V., Vatin, N.I. Ograzhdayushchaya konstruktsiya «nulevoy tolshchiny» – termopanel' [Zero-thickness building envelope - thermopanel]. Magazine of Civil Engineering. 2008. 1(1). Pp. 13–21. (rus)

25. Bronzova, M.K., Vatin, N.I., Garifullin, M.R. Frame buildings construction using monolithic foamed concrete. Construction of Unique Buildings and Structures. 2015. 28(1). Pp. 74-90. (rus)

26. Vatin, N.I., Grinfeld, G.I., Okladnikova, O.N., Tulko, S.I. Soprotivleniye teploperedache ograzhdayushchikh konstruktsiy iz gazobetona s oblitsovkoy iz silikatnogo kirpicha [Resistance to heat transfer of aerated concrete enclosures with silicate brick cladding]. StroyPROFIl. 2007. No. 5(59). Pp. 28–32. (rus)

27. Rybakov, V.A., Gamayunova, O.S. The stress-strain state of frame constructions' elements from thin-walled cores. Construction of Unique Buildings and Structures. 2013. 12(7). Pp. 79-123. (rus). DOI: 10.18720/CUBS.12.10

28. Lalin, V., Rybakov, V., Sergey, A. The finite elements for design of frame of thin-walled beams. Applied mechanics and materials. 2014. Pp. 858–863.

29. Stamatovic, B., Korsun, A. Local data flow principles in porosity of materials. Applied mechanics and materials. 2015. Pp. 371–376.

30. Korsun, V., Korsun, A. The influence of precompression on strength and strain properties of concrete under the effect of elevated temperatures. Applied mechanics and materials. 2015. Pp. 469–474.

31. Akimov, L.I., Ilenko, N., Mizharev, R., Cherkashin, A., Vatin, N.I., Chumadova, L.I. Composite concrete modifier cm 02-10 and its IMPA. Matec web of conferences. 2016. Pp. 01022.

32. Frolov, A., Chumadova, L., Cherkashin, A., Akimov, L. Prospects of use and impact of nanoparticles on the properties of high-strength concrete. Applied mechanics and materials. 2014. Pp. 1416–1424.

33. Kornilov, T.A., Gerasimov, G.N. Naruzhnyye steny maloetazhnykh domov iz legkikh stalnykh tonkostennykh konstruktsiy dlya usloviy kraynego severa [External walls of low-rise buildings made of light steel thin-walled structures for conditions of the far north]. Zhilishchnoye stroitelstvo. 2016. No. 7. Pp. 20–24. (rus)

34. Danilov, N.D., Doktorov, I.A., Ambrosyev, V.V., Fedotov, P.A., Semenov, A.A. Issledovaniye teplozashchitnykh svoystv fragmenta steny v klimaticheskoy kamere [Study of the heat-shielding properties of a wall fragment in a climate chamber]. Promyshlennoye i grazhdanskoye stroitelstvo. 2013. No. 8. Pp. 17–19. (rus)

Contacts:

Vladimir Rybakov, fishermanoff@mail.ru

Irina Ananeva, irina.ananeva94@yandex.ru

Egor Pichugin, pichugin_egor93@mail.ru

Marsel Garifullin, marsel.garifullin@tuni.fi

Rybakov, V.A., Ananeva, I.A., Pichugin, E.D., Garifullin, M.

20